

Lepton flavor violation decays $\tau^- \rightarrow \mu^- P_1 P_2$ in the topcolor-assisted technicolor model and the littlest Higgs model with T parity

Wei Liu, Chong-Xing Yue, Jiao Zhang

Department of Physics, Liaoning Normal University, Dalian 116029, China*

Abstract

The new particles predicted by the topcolor-assisted technicolor ($TC2$) model and the littlest Higgs model with T -parity (called LHT model) can induce the lepton flavor violation (LFV) couplings at tree level or one loop level, which might generate large contributions to some LFV processes. Taking into account the constraints of the experimental data on the relevant free parameters, we calculate the branching ratios of the LFV decay processes $\tau^- \rightarrow \mu^- P_1 P_2$ with $P_1 P_2 = \pi^+ \pi^-$, $K^+ K^-$ and $K^0 \bar{K}^0$ in the context of these two kinds of new physics models. We find that the $TC2$ model and the LHT model can indeed produce significant contributions to some of these LFV decay processes.

*cxyue@lnnu.edu.cn

1. Introduction

In the standard model (SM), because of the unitary of the leptonic analog of Cabibbo-Kobayashi-Maskawa (CKM) mixing matrix and the masslessness of three neutrinos, the lepton flavor violation (LFV) processes are forbidden at tree level. Experimentally, the neutrinos acquire small mass for the observation of neutrino oscillations and the LFV processes are possible [1]. Thus, the LFV processes may provide good tests of new physics (NP) beyond the SM . This fact has lead to great amount of the theoretical efforts studying on the underlying NP in the leptonic flavor sector.

In the SM , the τ lepton is the most heavy particle in the leptonic sector, which is much more sensitive than the leptons e or μ to NP related to the flavor and mass generation problems [2]. The semileptonic τ decays related LFV are very interesting and needed to be studied, which could provide a better laboratory to search NP .

Experimentally, with a total data set now exceeding 1.1 ab^{-1} of integrated luminosity and a $e^+e^- \rightarrow \tau^+\tau^-$ cross-section at 10.58 GeV of 0.919 nb [3], B factories have recorded more than 10^9 tau pairs and contributed significant progress to tau lepton physics. The current experimental limits for the LFV decay processes $\tau^- \rightarrow \mu^- P_1 P_2$ at 90% C.L. have been fixed at [4, 5]:

$$Br(\tau^- \rightarrow \mu^- \pi^+ \pi^-) < 2.9 \times 10^{-7}, \quad (1)$$

$$Br(\tau^- \rightarrow \mu^- K^+ K^-) < 2.5 \times 10^{-7}, \quad (2)$$

$$Br(\tau^- \rightarrow \mu^- K^0 \bar{K}^0) < 3.4 \times 10^{-6}. \quad (3)$$

There are a lot of theoretical researches on the LFV τ decays in many possible extension of the SM . For example, the LFV τ decays have been studied in supersymmetry ($SUSY$) model [6, 7, 8, 9], the littlest Higgs model with T parity (called LHT model) [10, 11, 12], and others [13, 14, 15, 16]. In particular, the LFV τ decays $\tau \rightarrow l P_1 P_2$ ($l = \mu, e$) have been studied in Refs. [6, 9, 17, 18, 19]. However, so far, we have not found discussions on the LFV τ decay processes $\tau^- \rightarrow \mu^- P_1 P_2$ with $P_1 P_2 = \pi^+ \pi^-, K^+ K^-$ and $K^0 \bar{K}^0$ in the framework of the topcolor-assisted technicolor ($TC2$) model [20] as well as the LHT model [21]. These two models are popular and interesting NP models at

present and the experimental upper limits of the LFV decay processes $\tau^- \rightarrow \mu^- P_1 P_2$ have been improved to $\mathcal{O}(10^{-7})$ at 90% C.L. [4, 5]. So in this paper, we would like to consider the contributions of the $TC2$ model and the LHT model to the LFV decay processes $\tau^- \rightarrow \mu^- P_1 P_2$.

Among various kinds of dynamical electroweak symmetry breaking ($EWSB$) theories, the topcolor scenario is attractive because it can explain the large top quark mass and provide a possible $EWSB$ mechanism [22]. The $TC2$ model [20] is one of the phenomenologically viable models, which has all essential features of the topcolor scenario. This model predicts the existence of the nonuniversal gauge boson Z' and the top-Higgs h_t^0 . These new particles treat the third generation fermions differently from those in the first and second generations and thus can lead to the tree level flavor-changing (FC) couplings. Thus these new particles might give significant contributions to the LFV semileptonic decays $\tau^- \rightarrow \mu^- P_1 P_2$. Our numerical results show that the contributions of the scalar h_t^0 are much small, while the nonuniversal gauge boson Z' can enhance the branching ratio $Br(\tau^- \rightarrow \mu^- P_1 P_2)$ by several orders of magnitude.

The LHT model [21] is one of the attractive little Higgs models, it predicts the existence of the T-odd $SU(2)$ doublet fermions and new gauge bosons. These new fermions and gauge bosons can provide rich phenomenology at present or in future high energy collider experiments [23, 24, 25, 26, 27, 28, 29, 30]. Our numerical results show that the contributions of the LHT model can significantly enhance the branching ratio $Br(\tau^- \rightarrow \mu^- P_1 P_2)$, which might approach its experimental upper limit with reasonable values of the free parameters.

The structure of this paper is as follows. After briefly summarize the relevant couplings of new particles to ordinary particles arising from the $TC2$ model and the LHT model, we calculate the branching ratios of the LFV decay processes $\tau^- \rightarrow \mu^- P_1 P_2$ with $P_1 P_2 = \pi^+ \pi^-$, $K^+ K^-$ and $K^0 \bar{K}^0$ generated by these two kinds of NP models in sections 2 and 3, respectively. In our numerical estimation, we have taken into account the constraints of the current experimental data on the model-dependent free parameters and compared our numerical results with the current experimental up limits for $\tau^- \rightarrow \mu^- P_1 P_2$ in these

two sections. Our conclusions and discussions are given in section 4. In appendix A we give the explicit forms of the relevant form factors for the pseudoscalar mesons P_1 and P_2 . The explicit forms of the relevant functions for the $TC2$ and the LHT models are collected in appendixes B and C, respectively.

2. The $TC2$ model and the LFV τ decay processes $\tau^- \rightarrow \mu^- P_1 P_2$

In the $TC2$ model [22], topcolor interaction is not flavor-universal and mainly couples to the third generation fermions. It generally generates small contributions to $EWSB$ and gives rise to the main part of the top quark mass. Thus, the nonuniversal gauge boson Z' has large Yukawa couplings to the third generation fermions. Such features lead to large tree level FC couplings of the nonuniversal gauge boson Z' to ordinary fermions when one writes the interaction in the fermion mass eigen-basis.

The explicit form for the LFV couplings of the nonuniversal gauge boson Z' to ordinary leptons, which are related our calculation, can be written as [31, 32]:

$$L_{Z'}^{FC} = \frac{1}{2}g_1 K' Z'_\mu [\bar{\tau}_L \gamma^\mu \mu_L + 2\bar{\tau}_R \gamma^\mu \mu_R], \quad (4)$$

where g_1 is the ordinary hypercharge gauge coupling constant. K' is the mixing factor between the leptons τ and μ . The relevant flavor-diagonal (FD) couplings of Z' to ordinary fermions can be written as [20, 22, 31]:

$$\begin{aligned} L_{Z'}^{FD} = & -\sqrt{4\pi K_1} \left\{ Z'_\mu \left[\frac{1}{2}\bar{\tau}_L \gamma^\mu \tau_L - \bar{\tau}_R \gamma^\mu \tau_R \right] - \tan^2 \theta' Z'_\mu \left[\frac{1}{6}\bar{u}_L \gamma^\mu u_L + \frac{2}{3}\bar{u}_R \gamma^\mu u_R \right. \right. \\ & \left. \left. + \frac{1}{6}\bar{d}_L \gamma^\mu d_L - \frac{1}{3}\bar{d}_R \gamma^\mu d_R + \frac{1}{6}\bar{s}_L \gamma^\mu s_L - \frac{1}{3}\bar{s}_R \gamma^\mu s_R \right] \right\}, \end{aligned} \quad (5)$$

where K_1 is the coupling constant and θ' is the mixing angle with $\tan \theta' = g_1/\sqrt{4\pi K_1}$.

For the $TC2$ model, the extended gauge groups are broken at the TeV scale, which proposes that K' is an $O(1)$ free parameter. Its value can be generally constrained by the present experimental upper limits on the LFV processes $l_i \rightarrow l_j \gamma$ and $l_i \rightarrow l_j l_k l_l$. For example, for the LFV process $\mu \rightarrow 3e$, the decay width arisen from Z' exchange can be written as [33]:

$$\Gamma(\mu \rightarrow 3e) = \frac{25\alpha^5}{384\pi K_1^3 \cos^{10}\theta_W} \frac{m_\mu^5}{M_{Z'}^4} K'^2, \quad (6)$$

where θ_W is the Weinberg angle. The current experimental upper limit is $Br^{exp}(\mu \rightarrow 3e) \leq 1 \times 10^{-12}$ [34], which can give constraints to the free parameters of the *TC2* model. In our following numerical calculation, we will take into account these limits.

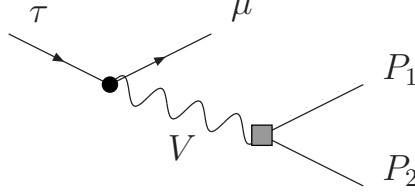


Figure 1: The Feynman diagrams contributing to the *LFV* decay processes

$\tau^- \rightarrow \mu^- P_1 P_2$. V represents a photon, a gauge boson or a Higgs boson.

From the above discussions, we can see that the nonuniversal gauge boson Z' can contribute to the *LFV* decay processes $\tau^- \rightarrow \mu^- P_1 P_2$ at tree level and one loop level as shown in Fig. 1. This diagram can be mediated by a photon, a gauge boson or a Higgs boson. Here the effective *LFV* vertex is represented by a black dot and the hadronic vertex by a gray box. There are also other types of diagrams induced by the gauge bosons W^\pm which have been discussed in Ref. [17]. However, those diagrams do not exist in our calculation, because they are just adapt to models including right-handed neutrinos. The pseudoscalar mesons P_1 and P_2 in the final state stem from the hadronisation of quark bilinear currents, namely parameterizing by the vector form factors $F^{P_1 P_2}(s)$ [8, 35]. These form factors can be defined through the vacuum-to- $P_1 P_2$ matrix elements of the local quark currents. The relevant formula can be written as [8, 35]:

$$\langle P_1 P_2 | \bar{q} \gamma_\mu q | 0 \rangle = (p_1 - p_2)_\mu F_q^{P_1 P_2}(s), \quad (7)$$

and $\sum_q^{u,d,s} Q_q F_q^{P_1 P_2}(s) = F^{P_1 P_2}(s)$, where Q_q is the electric charge of the q quark in units of the positron charge e and $s = (p_1 + p_2)^2$, in which p_1 and p_2 are the momentum of mesons P_1 and P_2 , respectively. The explicit forms of $F^{\pi^+ \pi^-}(s)$, $F^{K^+ K^-}(s)$ and $F^{K^0 \bar{K}^0}(s)$ have been displayed in the appendix A.

In this section, we give the explicit calculation of the Z' contributions to the *LFV* decay processes $\tau^- \rightarrow \mu^- P_1 P_2$ at both tree level and one loop level.

A. The tree level contributions of the nonuniversal gauge boson Z'

From Eq. (4), we can see that the nonuniversal gauge boson Z' can contribute to the LFV decay processes $\tau^- \rightarrow \mu^- P_1 P_2$ at tree level. The relevant Feynman diagram is similar to Fig. 1. The amplitude mediated by Z' exchange in terms of the final state quarks can be written as:

$$A_{Z'} = \frac{1}{M_{Z'}^2} C_{Z'} \bar{\mu} \gamma_\mu (v_l + a_l \gamma_5) \tau \bar{q} \gamma_\nu (v_q + a_q \gamma_5) q, \quad (8)$$

in which $v_{l(q)}$ and $a_{l(q)}$ are the constants for the vector and axial-vector couplings of the gauge boson Z' to ordinary leptons (quarks). The coefficient $C_{Z'}$ can be written as:

$$C_{Z'} = \frac{1}{2} g_1 K' \sqrt{4\pi K_1} \tan^2 \theta'. \quad (9)$$

Utilizing the hadronisation formula given by Eq. (7), the quark bilinear currents can be written in term of the form factors $F_q^{P_1 P_2}(s)$ which correspond to the two mesons P_1 and P_2 in the final state. Then, in terms of the final state hadrons, we can obtain the amplitude of the LFV decay processes $\tau^- \rightarrow \mu^- P_1 P_2$ generated by the nonuniversal gauge boson Z'

$$A_{Z'} = \frac{v_q}{M_{Z'}^2} C_{Z'} F_q^{P_1 P_2}(s) \bar{\mu} (\not{p}_1 - \not{p}_2) (v_l + a_l \gamma_5) \tau. \quad (10)$$

The explicit form of the branching ratio $Br(\tau^- \rightarrow \mu^- P_1 P_2)$ can be expressed as [8]:

$$Br(\tau^- \rightarrow \mu^- P_1 P_2) = \frac{\tau_\tau}{64\pi^3 m_\tau^2} \int_{s_{min}}^{s_{max}} ds \int_{t_{min}}^{t_{max}} dt |A_{Z'}|^2, \quad (11)$$

where τ_τ is the lifetime of lepton τ , $t = (p_\tau - p_1)^2$, and

$$\begin{aligned} t_{min}^{max} &= \frac{1}{4s} \left[(m_\tau^2 - m_\mu^2)^2 - (\lambda^{1/2}(s, m_P^2, m_P^2) \mp \lambda^{1/2}(m_\tau^2, s, m_\mu^2))^2 \right], \\ s_{min} &= 4m_P^2, \quad s_{max} = (m_\tau - m_\mu)^2, \quad \lambda(x, y, z) = (x + y - z)^2 - 4xy. \end{aligned} \quad (12)$$

In above equations we have assumed $m_{P_1} = m_{P_2} = m_P$.

Before giving numerical results, we need to specify the relevant SM parameters. Most of these input parameters are shown in Table 1. The vacuum tilting, the constraints from Z-pole physics, and U(1) triviality require $K_1 \leq 1$ [36]. The mass of nonuniversal gauge boson $M_{Z'}$ can be generally seen as free parameter. The lower bounds on $M_{Z'}$

$G_F = 1.166 \times 10^{-5} \text{ GeV}^{-2}$	$m_\tau = 1.78 \text{ GeV}$
$\alpha = 7.297 \times 10^{-3}$	$m_\mu = 0.106 \text{ GeV}$
$\tau_\tau = 2.91 \times 10^{-13} \text{ s}$	$m_K = 0.494 \text{ GeV}$
$m_\pi = 0.139 \text{ GeV}$	$m_{K^0} = 0.498 \text{ GeV}$
$M_W = 80.43 \text{ GeV}$	$\sin^2 \theta_W = 0.2315$

Table 1: Numerical inputs used in our analysis. Unless explicitly specified, they are taken from the Particle Data Group [5].

can be obtained from dijet and dilepton production in the Tevatron experiments [37] or $B\bar{B}$ mixing [38]. However, these bounds are significantly weaker than those from the precision electroweak data. Ref. [39] has shown that, to fit the precision electroweak data, the Z' mass $M_{Z'}$ must be larger than 1 TeV. In the following numerical estimation, we will assume that the values of the free parameters $M_{Z'}$ and K_1 are in the ranges of 1000 GeV \sim 2000 GeV and 0 \sim 1, respectively.

The branching ratios $Br(\tau^- \rightarrow \mu^- P_1 P_2)$ with $P_1 P_2 = \pi^+ \pi^-$, $K^+ K^-$ and $K^0 \bar{K}^0$ contributed by the nonuniversal gauge boson Z' at tree level are plotted as functions of the mass parameter $M_{Z'}$ in Fig. 2, in which we have taken $K_1 = 0.4$ (Fig. 2a) and 0.8 (Fig. 2b), and considered the constraints on the free parameter K' giving by the current experimental upper limit of $Br^{exp}(\mu \rightarrow 3e)$, as shown in Eq. (6). From these diagrams we can see that the values of the branching ratios $Br(\tau^- \rightarrow \mu^- \pi^+ \pi^-)$, $Br(\tau^- \rightarrow \mu^- K^+ K^-)$ and $Br(\tau^- \rightarrow \mu^- K^0 \bar{K}^0)$ decrease as the mass parameter $M_{Z'}$ increasing. It is obviously that the branching ratios of the different decay channels satisfy the relation $Br(\tau^- \rightarrow \mu^- \pi^+ \pi^-) > Br(\tau^- \rightarrow \mu^- K^+ K^-) \gtrsim Br(\tau^- \rightarrow \mu^- K^0 \bar{K}^0)$. This is mainly because the mass of the K meson is larger than that of the π meson and the FD couplings of the nonuniversal gauge boson Z' to up-type quarks are different from those for the down-type quarks as

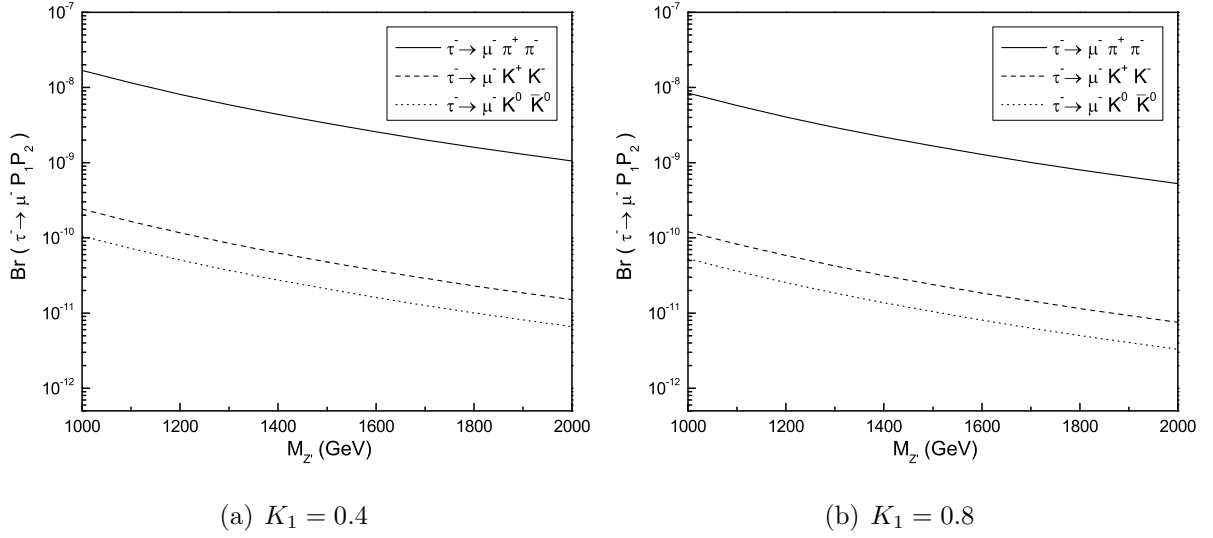


Figure 2: The branching ratios $Br(\tau^- \rightarrow \mu^- P_1 P_2)$ contributed by the nonuniversal gauge boson Z' at tree level as functions of mass parameter $M_{Z'}$ for the parameter $K_1 = 0.4$ (a) and $K_1 = 0.8$ (b).

shown in Eq. (5). The max values of the branching ratios for the LFV decay processes $\tau^- \rightarrow \mu^- K^+ K^-$ and $\tau^- \rightarrow \mu^- K^0 \bar{K}^0$ can reach 2.41×10^{-10} and 1.05×10^{-10} , respectively. However, these values are much smaller than the corresponding experimental upper limits given in Eqs. (2, 3). While the max value for the LFV decay process $\tau^- \rightarrow \mu^- \pi^+ \pi^-$ can reach 1.68×10^{-8} , which might approach its upper limit in the future high energy collider experiments.

B. The loop level contributions of the nonuniversal gauge boson Z'

The nonuniversal gauge boson Z' predicted by the $TC2$ model can also generate contributions to the LFV decay processes $\tau^- \rightarrow \mu^- P_1 P_2$ at one loop level. The relevant Feynman diagrams for the effective LFV vertexes $Z\tau\bar{\mu}$ and $\gamma\tau\bar{\mu}$ have been displayed in Fig. 3.

The effective Hamilton for the LFV decay process $\tau^- \rightarrow \mu^- P_1 P_2$ including the contributions of Z' at one loop level has the form:

$$H = H_1 + H_2, \quad (13)$$

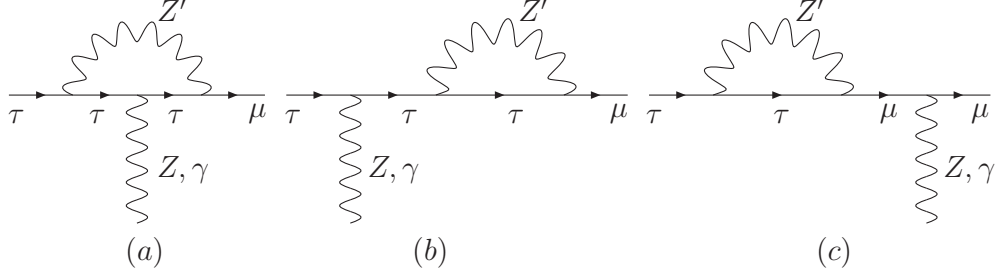


Figure 3: The Feynman diagrams for the effective LFV vertexes $Z\tau\bar{\mu}$ and $\gamma\tau\bar{\mu}$ contributed by the nonuniversal gauge boson Z' .

$$H_1 = \frac{G_F}{\sqrt{2}} \frac{\alpha}{2\pi \sin^2 \theta_W} C_1 \bar{\mu} \gamma_\mu (v_l + a_l \gamma_5) \tau \bar{q} \gamma_\nu (v_q + a_q \gamma_5) q, \quad (14)$$

$$H_2 = \frac{G_F}{\sqrt{2}} \frac{m_\tau e^2 Q_q}{4\pi^2 k^2} C_2 \bar{\mu} i \sigma_{\mu\nu} (v_l + a_l \gamma_5) \tau \bar{q} \gamma_\nu q, \quad (15)$$

where H_1 and H_2 represent the Z' contributions mediated by Z gauge boson exchange and the photon exchange, respectively. k represents the photon momentum. The explicit forms of the coefficients C_1 and C_2 are:

$$C_1 = \frac{2g_1 K' \sqrt{4\pi K_1}}{g_2^2} \left[4F_1(x_\tau) - 2F_2(x_\tau) + \left(1 + \frac{m_\tau}{m_\mu} F_3(x_\tau) \right) \right], \quad (16)$$

$$C_2 = \frac{32g_1 K' M_W^2 \sqrt{4\pi K_1}}{g_2^2 m_\tau} \left[F_4(x_\tau) + \left(1 + \frac{m_\tau}{m_\mu} F_3(x_\tau) \right) \right], \quad (17)$$

where g_2 is the SM $SU(2)_L$ gauge coupling constant. The Inami-Lim functions [40] $F_i(x)$ ($i = 1, 2, 3, 4$) are collected in Appendix B with $x_\tau = m_\tau^2/M_{Z'}^2$.

Applying similar hadronisation process to the bilinear quark currents as that for the tree level, the amplitude contributed by the nonuniversal gauge boson Z' at one loop can be written as:

$$A_1 = \frac{G_F}{\sqrt{2}} \frac{v_q \alpha}{2\pi \sin^2 \theta_W} C_1 F_q^{P_1 P_2}(s) \bar{\mu} (\not{p}_1 - \not{p}_2) (v_l + a_l \gamma_5) \tau, \quad (18)$$

$$A_2 = \frac{G_F}{\sqrt{2}} \frac{e^2 m_\tau}{2\pi^2 k^2} C_2 F^{P_1 P_2}(s) \bar{\mu} p_1^\mu \sigma_{\mu\nu} p_2^\nu (v_l + a_l \gamma_5) \tau. \quad (19)$$

In the context of the $TC2$ model, the expression of the corresponding branching ratio induced by the nonuniversal gauge boson Z' at one loop level can be written as:

$$Br(\tau^- \rightarrow \mu^- P_1 P_2) = \frac{\tau_\tau}{64\pi^3 m_\tau^2} \int_{s_{min}}^{s_{max}} ds \int_{t_{min}}^{t_{max}} dt (|A_1|^2 + |A_2|^2). \quad (20)$$

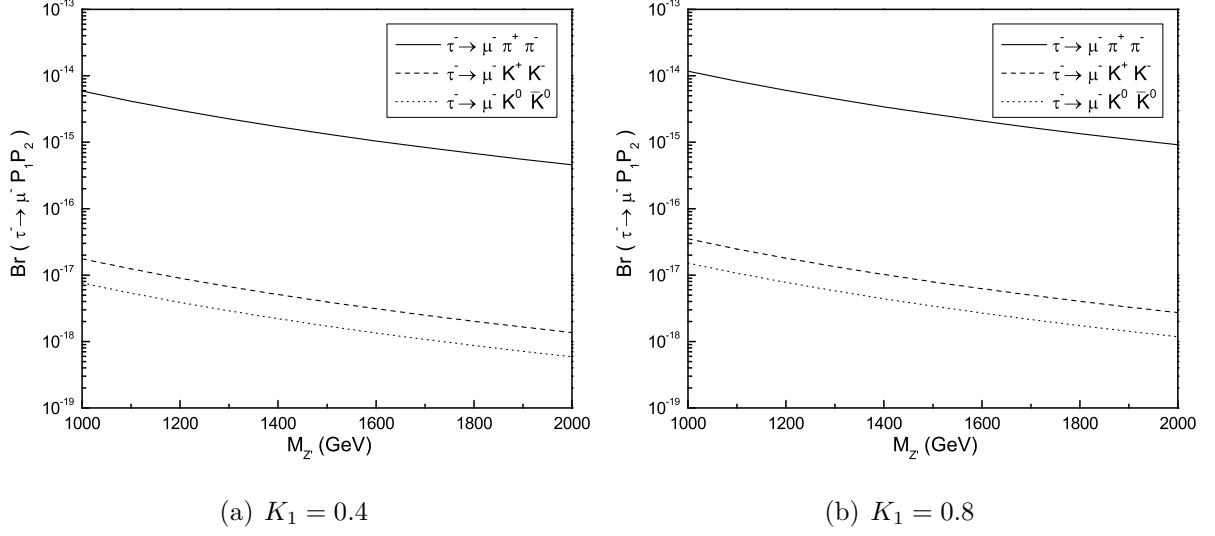


Figure 4: The branching ratios $Br(\tau^- \rightarrow \mu^- P_1 P_2)$ as functions of mass parameter $M_{Z'}$ at one loop level for the parameter $K_1 = 0.4$ (a) and $K_1 = 0.8$ (b).

Using the values of the relevant SM input parameters given at Table 1, we present the branching ratios $Br(\tau^- \rightarrow \mu^- \pi^+ \pi^-)$, $Br(\tau^- \rightarrow \mu^- K^+ K^-)$ and $Br(\tau^- \rightarrow \mu^- K^0 \bar{K}^0)$ contributed by the nonuniversal gauge boson Z' at one loop level as functions of the mass parameter $M_{Z'}$ in Fig. 4, in which we have taken $K_1 = 0.4$ (Fig. 4a) and 0.8 (Fig. 4b). From these diagrams, one can see that the values of the branching ratios $Br(\tau^- \rightarrow \mu^- \pi^+ \pi^-)$, $Br(\tau^- \rightarrow \mu^- K^+ K^-)$ and $Br(\tau^- \rightarrow \mu^- K^0 \bar{K}^0)$ decrease as the mass parameter $M_{Z'}$ increasing. The value of $Br(\tau^- \rightarrow \mu^- K^+ K^-)$ is close to that of $Br(\tau^- \rightarrow \mu^- K^0 \bar{K}^0)$ in most of the parameter space of the $TC2$ model. Comparing this figure to the Z' tree level contributions displayed in Fig. 2, one can see that the contributions of Z' to the LFV decay processes $\tau^- \rightarrow \mu^- \pi^+ \pi^-$, $\tau^- \rightarrow \mu^- K^+ K^-$ and $\tau^- \rightarrow \mu^- K^0 \bar{K}^0$ at one loop level are smaller than those of the tree level diagram by several orders of magnitude in most of the parameter space.

The $TC2$ model also predicts the existence of the top-Higgs h_t^0 , which treats the third generation fermions differently from those in the first and second generations and thus can lead to the tree level FC couplings to ordinary fermions. So this kind of new particle can also generate contributions to the LFV semileptonic decays $\tau^- \rightarrow \mu^- P_1 P_2$ at tree level

and one loop level. However, the LFV coupling $h_t^0 \tau \mu$ is suppressed by a factor m_τ/ν with the electroweak scale $\nu = 246$ GeV. Thus, the contributions of the top-Higgs h_t^0 to the LFV semileptonic decays $\tau^- \rightarrow \mu^- P_1 P_2$ are much smaller than those of the nonuniversal gauge boson Z' . Our numerical results show that it indeed is this case. The value of the branching ratio $Br(\tau^- \rightarrow \mu^- P_1 P_2)$ contributed by the scalar h_t^0 is smaller than that of Z' at least by two orders of magnitude.

3. The LHT model and the LFV τ decay process $\tau^- \rightarrow \mu^- P_1 P_2$

In this section, we first review the essential features of the LHT model studied in Ref. [21], which are related our calculation. Then we will consider the contributions of the LHT model to the LFV τ decay process $\tau^- \rightarrow \mu^- P_1 P_2$.

Similar with the LH model, the LHT model is based on an $SU(5)/SO(5)$ global symmetry breaking pattern. A subgroup $[SU(2) \times U(1)]_1 \times [SU(2) \times U(1)]_2$ of the $SU(5)$ global symmetry is gauged, and at the scale f it is broken into the SM electroweak symmetry $SU(2)_L \times U(1)_Y$. T-parity is an automorphism which exchanges the $[SU(2) \times U(1)]_1$ and $[SU(2) \times U(1)]_2$ gauge symmetries. The T-even combinations of the gauge fields are the SM electroweak gauge bosons W_μ^a and A_μ . The T-odd combinations are T-parity partners of the SM electroweak gauge bosons.

After taking into account $EWSB$, at the order of ν^2/f^2 , the masses of the T-odd set of the $SU(2) \times U(1)$ gauge bosons are given as:

$$M_{A_H} = \frac{g_1 f}{\sqrt{5}} \left[1 - \frac{5\nu^2}{8f^2} \right], \quad M_{Z_H} \approx M_{W_H} = g_2 f \left[1 - \frac{\nu^2}{8f^2} \right], \quad (21)$$

where f is the scale parameter of the gauge symmetry breaking of the LHT model. Because of the smallness of g_1 , the T-odd gauge boson A_H is the lightest T-odd particle, which can be seen as an attractive dark matter candidate [23, 41].

To avoid severe constraints and simultaneously implement T-parity, it is need to double the SM fermion doublet spectrum [21, 24]. The T-even combination is associated with the $SU(2)_L$ doublet, while the T-odd combination is its T-parity partner. The masses of the T-odd fermions can be written in a unified manner as:

$$M_{F_i} = \sqrt{2} k_i f, \quad (22)$$

where k_i are the eigenvalues of the mass matrix k and their values are generally dependent on the fermion species i .

The mirror fermions (T-odd quarks and T-odd leptons) have new flavor violating interactions with the SM fermions mediated by the new gauge bosons (A_H, W_H^\pm , or Z_H), which are parameterized by four CKM -like unitary mixing matrices, two for mirror quarks and two for mirror leptons [27, 28, 42]:

$$V_{Hu}, V_{Hd}, V_{Hl}, V_{H\nu}, \quad (23)$$

they satisfy:

$$V_{Hu}^+ V_{Hd} = V_{CKM}, \quad V_{H\nu}^+ V_{Hl} = V_{PMNS}, \quad (24)$$

where the CKM matrix V_{CKM} is defined through flavor mixing in the down-type quark sector, while the $PMNS$ matrix V_{PMNS} is defined through neutrino mixing. Similar with Ref. [28], we will set the Majorana phases of V_{PMNS} to zero in our following calculation. The matrix V_{Hl} can give rise to the LFV processes.

From the above discussions, we can see that the LHT model provides a new mechanism for the LFV processes, which comes from the flavor mixing in the mirror lepton sector. Thus, the LHT model might give significant contributions to the LFV processes $\tau^- \rightarrow \mu^- P_1 P_2$. The relevant Feynman diagrams have been shown in Fig. 5 and Fig. 6, in which we just display the effective LFV vertex without hadronic part. In these diagrams, l_H^i , ν_H^j and q_H^i represent the T-odd partners of three family leptons l_i , ν_j and quarks q_i , respectively. The Goldstone bosons ω^\pm , ω^0 and η are eaten by heavy gauge bosons W_H^\pm , Z_H and A_H , respectively. In this paper we use the 't Hooft-Feynman gauge, so the Goldstone Boson mass is the same as its corresponding gauge boson, that's to say: $M_\omega = M_{W_H}$, $M_{\omega^0} = M_{Z_H}$ and $M_\eta = M_{A_H}$. The relevant couplings of these new particles to ordinary leptons and their T-odd partners can be found in Ref. [28]. The effective Hamilton for the LFV decay process $\tau^- \rightarrow \mu^- P_1 P_2$ can be written as [28]:

$$H_3 = \frac{G_F}{\sqrt{2}} \frac{\alpha}{2\pi \sin^2 \theta_W} \bar{X}_{\text{odd}} \bar{\mu} \gamma_\mu (1 - \gamma_5) \tau \bar{q} \gamma_\nu (v_q + a_q \gamma_5) q, \quad (25)$$

$$H_4 = \frac{G_F}{\sqrt{2}} \frac{e^2 m_\tau Q_q}{4\pi^2 k^2} \bar{D}_{\text{odd}} \bar{\mu} i \sigma_{\mu\nu} k^\nu (1 + \gamma_5) \tau \bar{q} \gamma_\nu q, \quad (26)$$

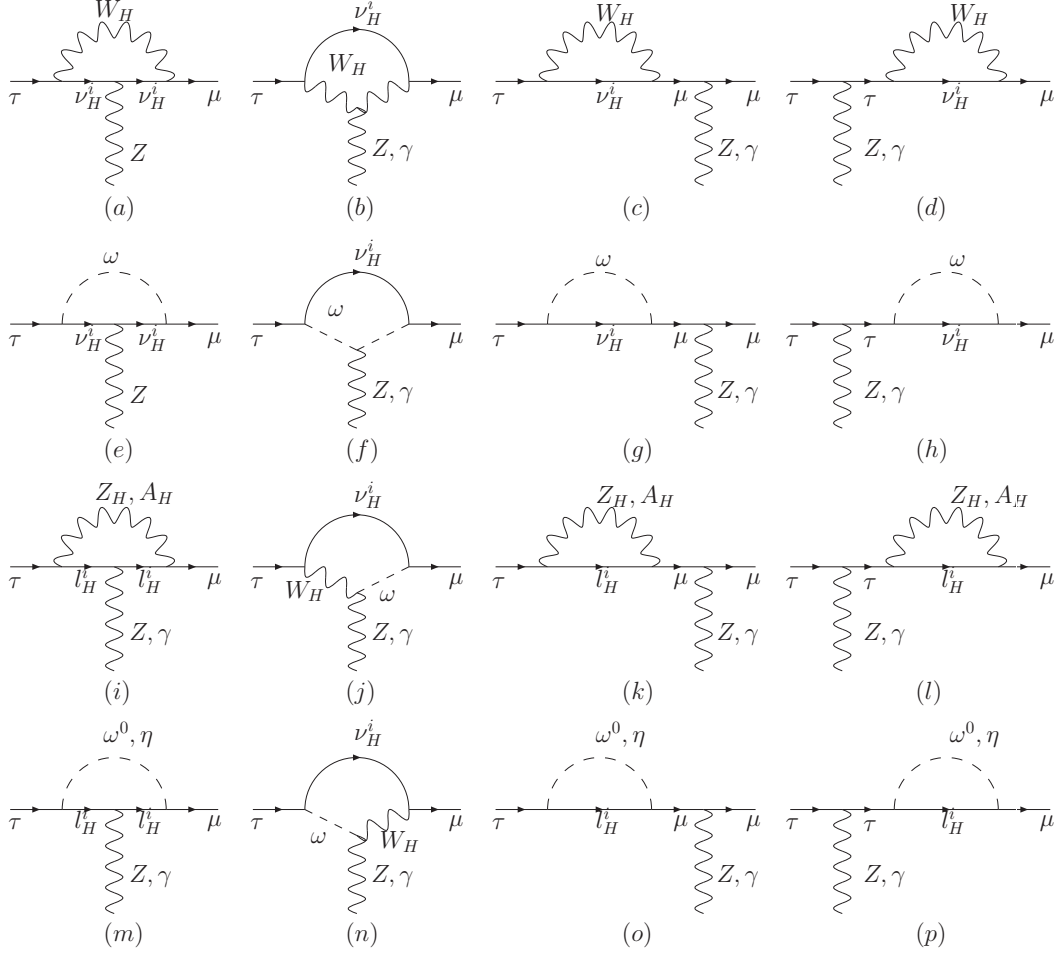


Figure 5: The penguin diagrams for the effective LFV vertexes $Z\tau\bar{\mu}$ and $\gamma\tau\bar{\mu}$ in the LHT model.

with

$$\bar{X}_{\text{odd}}^u = \left[\chi_2^{(\tau\mu)} (J^{u\bar{u}}(y_2, z) - J^{u\bar{u}}(y_1, z)) + \chi_3^{(\tau\mu)} (J^{u\bar{u}}(y_3, z) - J^{u\bar{u}}(y_1, z)) \right], \quad (27)$$

$$\bar{X}_{\text{odd}}^d = \left[\chi_2^{(\tau\mu)} (J^{d\bar{d}}(y_2, z) - J^{d\bar{d}}(y_1, z)) + \chi_3^{(\tau\mu)} (J^{d\bar{d}}(y_3, z) - J^{d\bar{d}}(y_1, z)) \right], \quad (28)$$

$$\bar{D}_{\text{odd}} = -\frac{\nu^2}{8f^2} \sum_i \chi_i^{\tau\mu} \left[D'_0(y_i) - \frac{7}{6} E'_0(y_i) - \frac{1}{10} E'_0(y'_i) \right], \quad (29)$$

here

$$J^{u\bar{u}}(y_i, z) = \frac{1}{64} \frac{v^2}{f^2} \left[y_i S_{\text{odd}}(y_i) + F^{u\bar{u}}(y_i, z; W_H) \right]$$

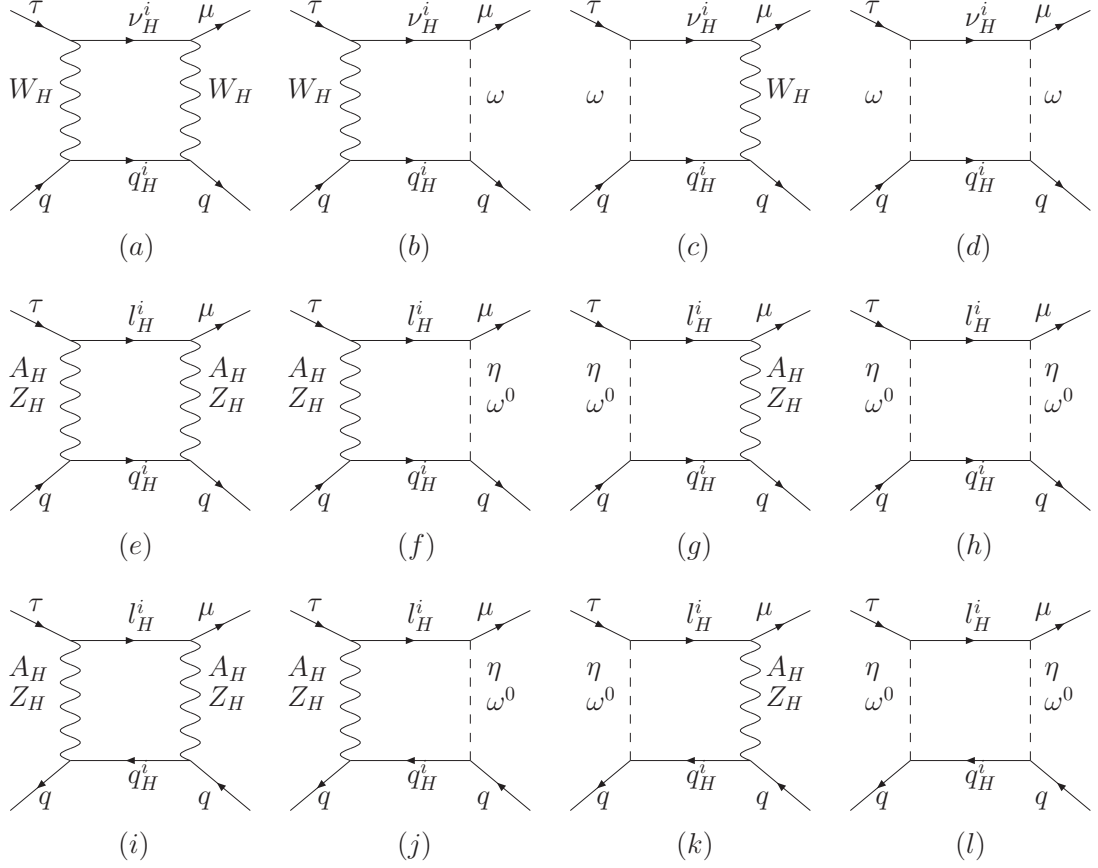


Figure 6: The box diagrams for the LFV decay process $\tau^- \rightarrow \mu^- P_1 P_2$ in the LHT model.

$$+4\left(G(y_i, z; Z_H) + G_1(y'_i, z'; A_H) - G_2(y_i, z; \eta)\right)\Big], \quad (30)$$

$$J^{d\bar{d}}(y_i, z) = \frac{1}{64} \frac{v^2}{f^2} \left[y_i S_{\text{odd}}(y_i) + F^{d\bar{d}}(y_i, z; W_H) - 4\left(G(y_i, z; Z_H) + G_1(y'_i, z'; A_H) + G_2(y_i, z; \eta)\right) \right], \quad (31)$$

where $y_i = M_{l_H}^2/M_{W_H}^2 = M_{l_H}^2/M_{Z_H}^2$, $z = m_{q_H}^2/M_{W_H}^2$, $y_i(z)' = 5y_i(z)/\tan^2\theta_W$, $\eta = \tan^2\theta_W/5$ and $\chi_i^{\tau\mu} = V_{Hl}^{*i\mu} V_{Hl}^{i\tau}$. The explicit forms of $S_{\text{odd}}(x)$, $F^{u,d}(x)$, $G_i(x)$, $D'_0(x)$ and $E'_0(x)$ are collected in Appendix C.

In the context of the LHT model, the amplitude of the LFV decay process $\tau^- \rightarrow$

$\mu^- P_1 P_2$ can be written as:

$$A_3 = \frac{G_F}{\sqrt{2}} \frac{v_q \alpha}{2\pi \sin^2 \theta_W} F_q^{P_1 P_2}(s) \bar{X}_{\text{odd}} \bar{\mu} (\not{p}_1 - \not{p}_2) (1 - \gamma_5) \tau, \quad (32)$$

$$A_4 = \frac{G_F}{\sqrt{2}} \frac{e^2 m_\tau}{2\pi^2 k^2} F^{P_1 P_2}(s) \bar{D}_{\text{odd}} \bar{\mu} i p_1^\mu \sigma_{\mu\nu} p_2^\nu (1 + \gamma_5) \tau. \quad (33)$$

The contributions of the *LHT* model to *LFV* decay process have been extensively studied and compared with the current experimental limits in the literatures [11, 12, 28, 29]. It has been shown that the *LHT* model can enhance the *SM* prediction values by several orders of magnitude and the experimental measurement data for some *LFV* decay processes can give constraints on the free parameters of the *LHT* model. For example, in order to suppress the branching ratio $Br(\mu \rightarrow e\gamma)$ and $Br(\mu \rightarrow 3e)$ predicted by the *LHT* model below the present experimental upper bounds, the relevant mixing matrix V_{Hl} must be rather hierarchical or mass splitting for the first and second T-odd lepton masses is very small. Ref.[28] has shown that there must be $\sin 2\theta \leq 0.05$ or $\delta \leq 5\%$. A complete analysis can be found in Ref.[28]. Thus, in our following numerical estimation, we will assume $M_{l_H^e} = M_{\nu_H^e} = M_{l_H^\mu} = M_{\nu_H^\mu} = M_1 = 800$ GeV, $V_{Hl} = V_{PMNS}^+$, and take $M_{l_H^\tau} = M_{\nu_H^\tau} = M_2$ and the scale parameter f as free parameters. Considering the mirror quarks only contribute to the branching ratios of decay $\tau^- \rightarrow \mu^- P_1 P_2$ in box diagrams, we assume their masses degeneration and take $M_{qH} = 1$ TeV.

The branching ratios $Br(\tau^- \rightarrow \mu^- P_1 P_2)$ with $P_1 P_2 = \pi^+ \pi^-$, $K^+ K^-$ and $K^0 \bar{K}^0$ contributed by the *LHT* model are plotted as functions of the scale parameter f for $M_2 = 500$ GeV (Fig. 7 (a)) and $M_2 = 1500$ GeV (Fig. 7 (b)). From these figures, one can see that the values of the branching ratios $Br(\tau^- \rightarrow \mu^- \pi^+ \pi^-)$, $Br(\tau^- \rightarrow \mu^- K^+ K^-)$ and $Br(\tau^- \rightarrow \mu^- K^0 \bar{K}^0)$ decrease as the scale parameter f increasing while as the mass of T-odd lepton $M_{l_H^\tau}$ decreasing. For $M_{l_H^\tau} = 1500$ GeV and $f = 500$ GeV, the value of the branching ratio $Br(\tau^- \rightarrow \mu^- \pi^+ \pi^-)$ can reach 3.14×10^{-8} , which is larger than that induced by the *TC2* model. For the *LFV* decay processes $\tau^- \rightarrow \mu^- K^+ K^-$ and $\tau^- \rightarrow \mu^- K^0 \bar{K}^0$, the values of their branching ratios are much smaller than the experimental upper limits in all of the parameter space of the *LHT* model.

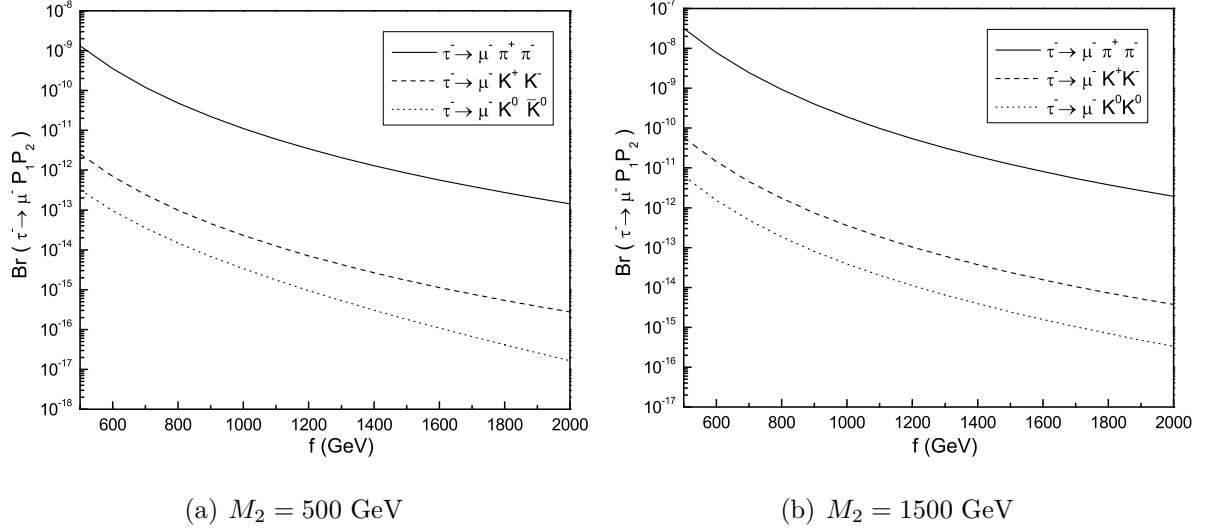


Figure 7: In the *LHT* model, the branching ratio $Br(\tau^- \rightarrow \mu^- P_1 P_2)$ as function of f for the parameter $M_2 = 500$ GeV (a), $M_2 = 1500$ GeV (b).

4. Conclusions and Discussions

The experimental upper limits of the *LFV* decay processes $\tau^- \rightarrow \mu^- P_1 P_2$ with $P_1 P_2 = \pi^+ \pi^-$, $K^+ K^-$ and $K^0 \bar{K}^0$ have been improved to $\mathcal{O}(10^{-7})$ at 90% C.L. [4, 5]. Whether these *LFV* decay processes exist or not is very important to the neutrino mass problem in the *SM*. It is well known that the *SM* does not allow the *LFV* processes at tree level, while many popular *NP* models can induce the *LFV* processes at tree level or loop level which might make their branching ratios significantly larger than those predicted by the *SM*. So the *LFV* decay processes $\tau^- \rightarrow \mu^- P_1 P_2$ are very suitable for the determination of the free parameters of the *NP* models. Studying of these decay processes are very interesting and needed.

The *TC2* model and the *LHT* model are two kinds of the popular *NP* models at present. In this paper, we have calculated their contributions to the branching ratios of the *LFV* decay processes $\tau^- \rightarrow \mu^- P_1 P_2$. We find that the new particles predicted by these two *NP* models can indeed produce significant contributions to these *LFV* decay processes. Taking into account the limits of the relevant experimental data on the free parameters, we calculate the $Br(\tau^- \rightarrow \mu^- P_1 P_2)$, and have the following conclusions.

i) The *TC2* model can induce the *LFV* decay processes $\tau^- \rightarrow \mu^- P_1 P_2$ both at tree level and one loop level, while the *LHT* model can only give contributions to these processes at one loop level. Furthermore, in the case of that the T-odd leptons are degenerate, the *LHT* model has no contributions to these *LFV* decay processes.

ii) For these two *NP* models, the branching ratios satisfy the following hierarchy: $Br(\tau^- \rightarrow \mu^- \pi^+ \pi^-) > Br(\tau^- \rightarrow \mu^- K^+ K^-) \gtrsim Br(\tau^- \rightarrow \mu^- K^0 \bar{K}^0)$.

iii) The contributions of the nonuniversal gauge boson Z' at tree level to the *LFV* decay processes $\tau^- \rightarrow \mu^- \pi^+ \pi^-$, $\tau^- \rightarrow \mu^- K^+ K^-$ and $\tau^- \rightarrow \mu^- K^0 \bar{K}^0$ are larger than those at one loop level by one order of magnitude in most of the parameter space. However, these values are still not large enough to be detected by present high energy experiments, which still need the future experimental verification.

iv) The branching ratios of the *LFV* decay processes $\tau^- \rightarrow \mu^- P_1 P_2$ generated by the *LHT* model are much larger than those generated by the *TC2* model. For $M_{l_H} = 1500$ GeV and $f = 500$ GeV, the value of the branching ratio $Br(\tau^- \rightarrow \mu^- \pi^+ \pi^-)$ can reach 3.14×10^{-8} , which might approach the upper limit given in Eqs. (1). However, the values of the branching ratios of the *LFV* decay processes $\tau^- \rightarrow \mu^- K^+ K^-$ and $\tau^- \rightarrow \mu^- K^0 \bar{K}^0$ are smaller than 1×10^{-9} in most of parameter space of the *LHT* model.

Our calculation can be extended to the *LFV* decay process $\tau^- \rightarrow e^- P_1 P_2$ by replacing the mass parameter m_μ to m_e . Since the nonuniversal gauge boson Z' treats the first generation fermions same as those in the second generation, the coefficient of the coupling $Z'\tau\mu$ approximately equals to that of the coupling $Z'\tau e$. This feature leads to the fact that the contribution of the *TC2* model to the decay $\tau^- \rightarrow e^- P_1 P_2$ is nearly the same as that of the decay $\tau^- \rightarrow \mu^- P_1 P_2$ channel. For the *LHT* model, its contributions to the *LFV* decay processes $\tau^- \rightarrow e^- (\mu^-) P_1 P_2$ can only exist at one loop. The relevant flavour mixing matrix elements and the masses of new particles for the *LFV* decay process $\tau^- \rightarrow e^- P_1 P_2$ are different from those of the *LFV* decay process $\tau^- \rightarrow \mu^- P_1 P_2$, which can make the branching ratios of these two decay processes different from each other. However, if we neglect these differences, the value of the branching ratio for the decay process $\tau^- \rightarrow \mu^- P_1 P_2$ should approximately equals to that of the decay process $\tau^- \rightarrow e^- P_1 P_2$.

Acknowledgments

This work was supported in part by the National Natural Science Foundation of China under Grants No.10675057 and 10975067, Specialized Research Fund for the Doctoral Program of Higher Education(SRFDP) (No.200801650002), the Natural Science Foundation of the Liaoning Scientific Committee(No.20082148), and Foundation of Liaoning Educational Committee(No.2007T086).

Appendix

A. The relevant functions of the hadronic form factors

In this appendix we list the hadronic form factors that are related to the LFV τ decays $\tau^- \rightarrow \mu^- P_1 P_2$. Their explicit expressions have been given in Ref. [6], we just put the related functions as follows:

$$F^{\pi^+\pi^-}(s) = F(s) \exp \left[2 \operatorname{Re} \left(\tilde{H}_{\pi\pi}(s) \right) + \operatorname{Re} \left(\tilde{H}_{KK}(s) \right) \right], \quad (34)$$

$$F^{K^+K^-}(s) = F_\rho(s) + F_\omega(s) + F_\phi(s), \quad (35)$$

$$F^{K^0\bar{K}^0}(s) = -F_\rho(s) + F_\omega(s) + F_\phi(s), \quad (36)$$

with

$$\begin{aligned} F(s) &= \frac{M_\rho^2}{M_\rho^2 - s - iM_\rho\Gamma_\rho(s)} \left[1 + \left(\delta \frac{M_\omega^2}{M_\rho^2} - \gamma \frac{s}{M_\rho^2} \right) \frac{s}{M_\omega^2 - s - iM_\omega\Gamma_\omega} \right] \\ &\quad - \frac{\gamma s}{M_{\rho'}^2 - s - iM_{\rho'}\Gamma_{\rho'}(s)}, \\ F_\rho(s) &= \frac{1}{2} \frac{M_\rho^2}{M_\rho^2 - s - iM_\rho\Gamma_\rho(s)} \exp \left[2 \operatorname{Re} \left(\tilde{H}_{\pi\pi}(s) \right) + \operatorname{Re} \left(\tilde{H}_{KK}(s) \right) \right], \\ F_\omega(s) &= \frac{1}{2} \left[\sin^2 \theta_V \frac{M_\omega^2}{M_\omega^2 - s - iM_\omega\Gamma_\omega} \right] \exp \left[3 \operatorname{Re} \left(\tilde{H}_{KK}(s) \right) \right], \\ F_\phi(s) &= \frac{1}{2} \left[\cos^2 \theta_V \frac{M_\phi^2}{M_\phi^2 - s - iM_\phi\Gamma_\phi} \right] \exp \left[3 \operatorname{Re} \left(\tilde{H}_{KK}(s) \right) \right], \\ \Gamma_\rho(s) &= \frac{M_\rho s}{96\pi F^2} \left[\sigma_\pi^3(s) \theta(s - 4m_\pi^2) + \frac{1}{2} \sigma_K^3(s) \theta(s - 4m_K^2) \right], \\ \Gamma_{\rho'}(s) &= \Gamma_{\rho'}(M_{\rho'}^2) \frac{s}{M_{\rho'}^2} \left(\frac{\sigma_\pi^3(s) + \frac{1}{2} \sigma_K^3(s) \theta(s - 4m_K^2)}{\sigma_\pi^3(M_{\rho'}^2) + \frac{1}{2} \sigma_K^3(M_{\rho'}^2) \theta(s - 4m_K^2)} \right) \theta(s - 4m_\pi^2). \end{aligned} \quad (37)$$

where $\sigma_P(s) = \sqrt{1 - 4\frac{m_P^2}{s}}$, and the other definitions are:

$$\begin{aligned}
\beta &= \frac{\Theta_{\rho\omega}}{3M_\rho^2}, \\
\gamma &= \frac{F_V G_V}{F^2} (1 + \beta) - 1, \\
\delta &= \frac{F_V G_V}{F^2} - 1, \\
\tilde{H}_{PP}(s) &= \frac{s}{F^2} M_P(s), \\
M_P(s) &= \frac{1}{12} \left(1 - 4\frac{m_P^2}{s} \right) J_P(s) - \frac{k_P(M_\rho)}{6} + \frac{1}{288\pi^2}, \\
J_P(s) &= \frac{1}{16\pi^2} \left[\sigma_P(s) \ln \frac{\sigma_P(s) - 1}{\sigma_P(s) + 1} + 2 \right], \\
k_P(\mu) &= \frac{1}{32\pi^2} \left(\ln \frac{m_P^2}{\mu^2} + 1 \right).
\end{aligned} \tag{38}$$

The contribution of the isospin breaking $\rho - \omega$ mixing $\Theta_{\rho\omega} = -3.3 \times 10^{-3} \text{ GeV}^2$, and the asymptotic constraint on the $N_C \rightarrow \infty$ vector form factor indicates $F_V G_V \simeq F^2 = F_\pi^2$. The mixing between the octet and singlet vector components employed in the construction of the $I = 0$ component of the kaon vector form factors is defined by :

$$\begin{pmatrix} \phi \\ \omega \end{pmatrix} = \begin{pmatrix} \cos \theta_V & -\sin \theta_V \\ \sin \theta_V & \cos \theta_V \end{pmatrix} \begin{pmatrix} v_8 \\ v_0 \end{pmatrix}, \tag{39}$$

and the ideal mixing $\theta_V = 35^\circ$ was used.

B. The relevant functions in the $TC2$ model

In the framework of $TC2$ model, the Inami-Lim functions that are used in our calculation are given as following.

$$F_1(x) = \frac{1}{8} \left[\frac{x^2 \ln x}{(x-1)^2} - \frac{2x \ln x}{(x-1)^2} + \frac{x}{x-1} \right]; \tag{40}$$

$$F_2(x) = -\frac{1}{4} \left[\frac{x}{x-1} - \frac{x \ln x}{(x-1)^2} \right]; \tag{41}$$

$$\begin{aligned}
F_3(x) &= \frac{1}{32} \left[\frac{x^2 \ln x}{(x-1)^2} - \frac{x}{x-1} - \frac{x \gamma_E}{2} - x \ln 4\pi - \frac{3x^2}{8} \right. \\
&\quad \left. + \frac{x^4 \ln x}{4(x-1)^2} - \frac{x^2}{4(x-1)} \right];
\end{aligned} \tag{42}$$

$$F_4(x) = -\frac{x}{16} \left[\frac{-1}{4(x-1)} + \frac{3}{4(x-1)^2} + \frac{3}{2(x-1)^3} - \frac{3x \ln x}{(x-1)^4} \right]. \quad (43)$$

C. The relevant functions in the LHT model

In this appendix we enumerate the functions related our calculation of the LFV τ decays $\tau^- \rightarrow \mu^- P_1 P_2$ in the LHT model, which have been discussed in Ref. [28].

$$S_{odd}(x) = \frac{x^2 - 2x + 4}{(1-x)^2} \ln x + \frac{7-x}{2(1-x)}, \quad (44)$$

$$F^{u\bar{u}}(y_i, z; W_H) = \frac{3}{2} y_i - F_5(y_i, z) - 7F_6(y_i, z) - 9U(y_i, z), \quad (45)$$

$$F^{d\bar{d}}(y_i, z; W_H) = \frac{3}{2} y_i - F_5(y_i, z) - 7F_6(y_i, z) + 3U(y_i, z), \quad (46)$$

$$F_5(y_i, z) = \frac{y_i^3 \log y_i}{(1-y_i)(z-y_i)} + \frac{z^3 \log z}{(1-z)(y_i-z)}, \quad (47)$$

$$F_6(y_i, z) = - \left[\frac{y_i^2 \log y_i}{(1-y_i)(z-y_i)} + \frac{z^2 \log z}{(1-z)(y_i-z)} \right], \quad (48)$$

$$U(y_i, z) = \frac{y_i^2 \log y_i}{(y_i-z)(1-y_i)^2} + \frac{z^2 \log z}{(z-y_i)(1-z)^2} + \frac{1}{(1-y_i)(1-z)} \quad (49)$$

$$G(y_i, z; Z_H) = -\frac{3}{4} U(y_i, z), \quad (50)$$

$$G_1(y'_i, z'; A_H) = \frac{1}{25a} G(y'_i, z'; Z_H), \quad (51)$$

$$G_2(y_i, z; \eta) = -\frac{3}{10a} \left[\frac{y_i^2 \log y_i}{(1-y_i)(\eta-y_i)(y_i-z)} + \frac{z^2 \log z}{(1-z)(\eta-z)(z-y_i)} + \frac{\eta^2 \log \eta}{(1-\eta)(y_i-\eta)(\eta-z)} \right], \quad (52)$$

$$D'_0(x) = -\frac{3x^3 - 2x^2}{2(x-1)^4} \ln x + \frac{8x^3 + 5x^2 - 7x}{12(x-1)^3}, \quad (53)$$

$$E'_0(x) = \frac{3x^2}{2(x-1)^4} \ln x + \frac{x^3 - 5x^2 - 2x}{4(x-1)^3}. \quad (54)$$

References

- [1] For recent reviews, see e.g., V. Barger, D. Marfatia, and K. Whisnant, *Int. J. Mod. Phys. E***12**, 569(2003); B. Kayser, p. 145 of the Review of Particle Physics, *Phys. Lett. B***592**, 1(2004); M. C. Gonzalez-Garcia and M. Maltoni, *Phys. Rept.***460**, 1(2008); R. N. Mohapatra and A. Y. Smirnov, *Ann. Rev. Nucl. Part. Sci.***56**, 569(2006); A.

- Strumia and F. Vissani, arXiv:hep-ph/0606054; Z. Z. Xing, *Int. J. Mod. Phys. A***23**, 4255(2008).
- [2] A. Pich, *Nucl. Phys. Proc. Suppl.***98**, 385(2001); M. Davier, A. Hocker, Z. Q. Zhang, *Rev. Mod. Phys.***78**, 1043(2006).
- [3] S. Banerjee, B. Pietrzyk, J. M. Roney, and Z. Was, *Phys. Rev. D***77**, 054012(2008).
- [4] B. Aubert et al. [BaBar Collaboration], *Phys. Rev. Lett.***95**, 191801(2005); Y. Yusa et al. [BELLE Collaboration], *Phys. Lett. B***640**, 138(2006).
- [5] W. M. Yao et al. [Particle Data Group], *J. Phys. G***33**, 1 (2006) and 2007 partial update for 2008 edition.
- [6] E. Arganda, M. J. Herrero, J. Portoles, *JHEP***0806**, 079(2008).
- [7] A. Brignole, A. Rossi, *Nucl. Phys. B***701**, 3(2004).
- [8] C. H. Chen, C. Q. Geng, *Phys. Rev. D***74**, 035010(2006).
- [9] T. Fukuyama, A. Ilakovac, T. Kikuchi, *Eur. Phys. J. C***56**, 125(2008).
- [10] A. Goyal, arXiv:hep-ph/0609095.
- [11] S. R. Choudhury, A. S. Cornell, A. Deandrea, N. Gaur, A. Goyal, *Phys. Rev. D***75**, 055011(2007).
- [12] M. Blanke, A. J. Buras, B. Duling, A. Poschenrieder, C. Tarantino, *JHEP***0705**, 013(2007).
- [13] C. X. Yue, L. H. Wang, W. Ma, *Phys. Rev. D***74**, 115018(2006); Z. H. Li, Y. Li, H. X. Xu, *Phys. Lett. B***677**, 150(2009).
- [14] X. G. He, S. Oh, *JHEP***0909**, 027(2009); A. Arhrib, R. Benbrik, C. H. Chen, arXiv:0903.1553.
- [15] A. G. Akeroyd, M. Aoki, Y. Okada, *Phys. Rev. D***76**, 013004(2007).

- [16] W. J. Li, Y. D. Yang, X. D. Zhang, *Phys. Rev. D***73**, 073005(2006); W. J. Li, Y. Q. Ma, G. W. Liu, W. Guo, arXiv:0812.0727.
- [17] A. Ilakovac, *Phys. Rev. D***54**, 5653(1996).
- [18] V. Gribov, S. Kovalenko and I. Schmidt, *Nucl. Phys. B***607**, 355(2001).
- [19] A. Atre, V. Barger and T. Han, *Phys. Rev. D***71**, 113014(2005).
- [20] C. T. Hill, *Phys. Lett. B***345**, 483(1995); K. D. Lane and E. Eichten, *Phys. Lett. B***352**, 382(1995); K. D. Lane, *Phys. Lett. B***433**, 96(1998); G. Cvetič, *Rev. Mod. Phys.***71**, 513(1999).
- [21] H. C. Cheng, I. Low, *JHEP***0309**, 051(2003); *JHEP***0408**, 061(2004); I. Low, *JHEP***0410**, 067(2004).
- [22] C. T. Hill and E. H. Simmons, *Phys. Rept.***381**, 235(2003); **390**, 553(E)(2004).
- [23] C. S. Chen, K. Cheung and T. C. Yuan, *Phys. Lett. B***644**, 158(2007).
- [24] J. Hubisz, P. Meade, *Phys. Rev. D***71**, 035016(2005); J. Hubisz, P. Meade, A. Noble and M. Perelstein, *JHEP***0601**, 135(2006).
- [25] C. R. Chen, K. Tobe, C. P. Yuan, *Phys. Lett. B***640**, 263(2006); A. Belyaev, C. R. Chen, K. Tobe, C. P. Yuan, *Phys. Rev. D***74**, 115020(2006); C. X. Yue, L. Ding, J. Y. Liu, *Phys. Rev. D***77**, 115003(2008); C. X. Yue, H. D. Yang, W. Ma, *Nucl. Phys. B***818**, 1(2009).
- [26] Q. H. Cao, C. S. Li, C. P. Yuan, *Phys. Lett. B***668**, 24(2008); D. Choudhury, D. K. Ghosh, *JHEP***0708**, 084(2007); S. Matsumoto, M. M. Nojiri, D. Nomura, *Phys. Rev. D***75**, 055006(2007); K. Kong, S. C. Park, *JHEP***0708**, 038(2007); C. X. Yue, N. Zhang, S. H. Zhu, *Eur. Phys. J. C***53**, 215(2008).
- [27] A. Freitas, D. Wyler, *JHEP***0611**, 061(2006); M. Blanke et al, *JHEP***0612**, 003(2006).

- [28] F. del Aguila, J. I. Illana, M. D. Jenkins, *JHEP***0901**, 080(2009); M. Blanke et al., arXiv:0906.5454; M. Blanke et al., *JHEP***0701**, 066(2007).
- [29] C. X. Yue, J. Y. Liu, S. H. Zhu, *Phys. Rev. D***78**, 095006(2008).
- [30] L. Wang, W. Y. Wang, J. M. Yang, H. J. Zhang, *Phys. Rev. D***76**, 017702(2007);
X. L. Wang, Y. Y. Zhang, H. L. Jin, Y. H. Xi, *Nucl. Phys. B***810**, 226(2009).
- [31] G. Buchalla, G. Burdman, C. T. Hill, and D. Kominis, *Phys. Rev. D***53**, 5185(1996).
- [32] C. X. Yue, Y. M. Zhang, L. J. Liu, *Phys. Lett. B***547**, 252(2002).
- [33] C. X. Yue, L. J. Liu, *Phys. Lett. B***564**, 55(2003).
- [34] M. L. Brooks et al. [MEGA Collaboration], *Phys. Rev. Lett.* **83**, 1521(1999).
- [35] H. Y. Cheng, C. K. Chua, A. Soni, *Phys. Rev. D***76**, 094006(2007); H. Y. Cheng, arXiv:0806.2895.
- [36] M. B. Popovic and E. H. Simmons, *Phys. Rev. D***58**, 095007(1998); G. Burdman and N. J. Evens, *Phys. Rev. D***59**, 115005(1999).
- [37] A. A. Andrianov, P. Osland, A. A. Pankov, N. V. Romanenko, J. Sirkka, *Phys. Rev. D***58**, 075001(1998); K. R. Lynch, S. Mrenna, M. Narain, E. H. Simmons, *Phys. Rev. D***63**, 035006(2001).
- [38] E. H. Simmons, *Phys. Lett. B***526**, 365(2002).
- [39] R. S. Chivukula and E. H. Simmons, *Phys. Rev. D***66**, 015006(2002).
- [40] T. Inami, C. S. Lim, *Prog. Theor. Phys.***65**, 297(1981); A. J. Buras, arXiv:hep-ph/9806471.
- [41] A. Birkedal, A. Noble, M. Perelstein, A. Spray, *Phys. Rev. D***74**, 035002(2006); M. Asano, S. Matsumoto, N. Okada, Y. Okada, *Phys. Rev. D***75**, 063506(2007); M. Perelstein, A. Spray, *Phys. Rev. D***75**, 083519(2007).

- [42] J. Hubisz, S. J. Lee, G. Paz, *JHEP***0606**, 041(2006); M. Blanke et al., *Phys. Lett. B***646**, 253(2007).